Role of the $-SiH_3$ Functional Group in Silane Adsorption and Dissociation on Si(100)

Jiazhan Xu,[†] W. J. Choyke,[‡] and John T. Yates, Jr.*,[†]

Surface Science Center, Department of Chemistry, University of Pittsburgh, Pittsburgh, Pennsylvania 15260, and Department of Physics, University of Pittsburgh, Pittsburgh, Pennsylvania 15260

Received: March 5, 1997; In Final Form: June 3, 1997[⊗]

The adsorption and reaction behavior of methylsilane (CH_3SiH_3) and disilane (Si_2H_6) on Si(100) single crystals has been studied using temperature-programmed desorption (TPD) and Auger electron spectroscopy (AES). It was found that CH_3SiH_3 and Si_2H_6 molecules have similar adsorption behavior while ethane (C_2H_6) does not stick on Si(100) at 90 K. These results indicate that $-SiH_3$ is the key functional group involved in silane adsorption. The adsorption coverage of CH_3SiH_3 at 90 K was found to be about twice as large as that at 300 K, indicating that methylsilane adsorbs dissociatively on Si(100) at 300 K with the breaking of the Si−C bond, producing enhanced dangling bond site blockage compared to the undissociated chemisorbed molecule. Based on the results, pentacoordinate silicon in $-SiH_3$ groups is postulated to be involved in the nondissociative chemisorption and in the S_N2 dissociative reaction of CH_3SiH_3 on dangling bond sites on Si(100).

I. Introduction

The reactivity of silane molecules with semiconductor surfaces to deposit silicon and/or silicon-containing thin films is fundamentally important in semiconductor technology. For example, there is interest in β-silicon carbide (β-SiC) film synthesis using methylsilane as a precursor.[1−4] For silanes containing a functional group other than the $-SiH_3$ group, the question arises as to the relative surface reactivity of this functional group compared to the reactivity of the $-SiH_3$ group. This paper provides insight into surface reactivity for the CH_3-SiH_3 molecule chemisorbing and decomposing on Si(100), where the $-SiH_3$ group is found to be the reactive functionality.

Our current knowledge of methylsilane adsorption and reaction on silicon surfaces is very limited. On the other hand, a similar molecule, disilane, has been studied extensively using various methods.[5] An accepted model is that Si_2H_6 adsorbs molecularly on Si(100) and Si(111) surfaces at low temperatures and that the Si−Si bond dissociates at temperatures above 120 K.[5,6] Recently, scanning tunneling microscope (STM) studies[7,8] revealed several different adsorbate features, corresponding to SiH_3, SiH_2, and SiH species, after disilane adsorption on Si(100) at 300 K at low coverages. At high coverages, a large fraction of SiH_3(a) species were observed immediately after adsorption. The stability of the chemisorbed SiH_3 species at higher coverages is probably related to the decreased number of the dangling bond (db) sites available for the further dissociation.[5]

In this study, CH_3SiH_3 adsorption and reaction on Si(100) were investigated by quantitatively comparing its behavior to the closely related molecules, C_2H_6 and Si_2H_6. It was found that C_2H_6 did not stick on Si(100) at 90 K while CH_3SiH_3 and Si_2H_6 molecules had similar initial sticking coefficients and saturation coverages, forming nondissociated chemisorbed species. These results alone suggest that $-SiH_3$ is the important functional group governing silane adsorption. By comparison of the saturation coverage of CH_3SiH_3 at 300 and 90 K, it is concluded that methylsilane adsorbs dissociatively at 300 K on Si(100) with the breaking of the Si−C bond. Based on the experimental results, an adsorption structure and a nucleophilic substitution reaction mechanism for CH_3SiH_3 dissociation on Si(100) are proposed that involve surface intermediates having pentacoordinate bonding at the Si atom in the $-SiH_3$ group.

II. Experimental Section

Experiments were performed in an ultrahigh vacuum (UHV) chamber with a base pressure of $\sim 5 \times 10^{-11}$ Torr as described previously.[9] Briefly, the UHV system contains facilities for Auger electron spectroscopy (AES), X-ray photoelectron spectroscopy (XPS), low-energy electron diffraction (LEED), and temperature-programmed desorption (TPD) measurement using an apertured quadrupole mass spectrometer. A heating rate of 3 K/s was used in all the TPD measurements.

Si(100) single crystals (1.5 mm thick, B-doped with conductivity of 10 Ω cm), obtained from Virginia Semiconductor, were mounted by two tantalum brackets with four silicon wafer spacers and two tantalum springs. The crystals were resistively heated, providing temperature uniformity along the sample (±15 K at 1400 K). Detailed mounting and temperature measurement studies with this form of mounting were described by Nishino et al.[10] Crystal cleaning was done by outgassing in vacuum at 950 K followed by heating to 1400 K. Surface cleanliness and ordering were checked by AES and LEED, respectively.

Methylsilane (99.9%) and disilane (99.998%) reagents were obtained from Voltaix, Inc., while ethane (98%) was obtained from Cambridge Laboratories. Several freeze−pump−thaw cycles were performed to further purify the reagents. The purities of the reagents were checked using a mass spectrometer in the UHV system.

The adsorbates were delivered to the single-crystal surface using a collimated and absolutely calibrated beam doser. The conductance of this doser was measured with CH_3SiH_3 and found to be 6.6×10^{12} molecules $Torr^{-1}$ s^{-1}. On the basis of the geometry of the doser and crystal, it was estimated that the fractional interception of the gas beam by the crystal was 0.4.[11,12]

III. Results

The adsorption and desorption behavior of CH_3SiH_3 and Si_2H_6 on Si(100) has been studied using TPD, as shown in Figure 1. In all the experiments, the Si(100) surface was exposed to $\sim 7 \times 10^{14}$ molecules/cm^2 at a specified temperature and then heated in vacuum at a heating rate of 3 K/s. The desorption species

[†] Department of Chemistry.
[‡] Department of Physics.
[⊗] Abstract published in *Advance ACS Abstracts,* July 15, 1997.

S1089-5647(97)00832-8 CCC: $14.00

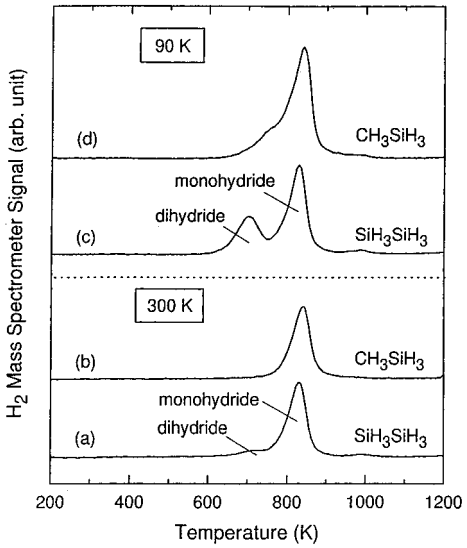

Figure 1. Temperature-programmed desorption study of CH_3SiH_3 and Si_2H_6 on Si(100) at 300 and 90 K. The heating rate was 3 K/s.

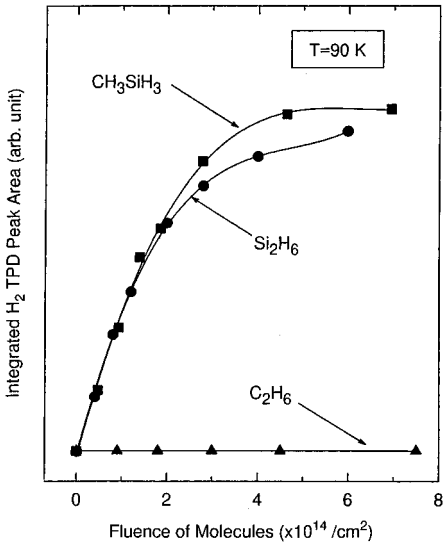

Figure 2. Comparison of C_2H_6, CH_3SiH_3, and Si_2H_6 adsorption on Si(100) at 90 K. The integrated H_2 desorption peak area was used to measure the relative coverage of the three molecules.

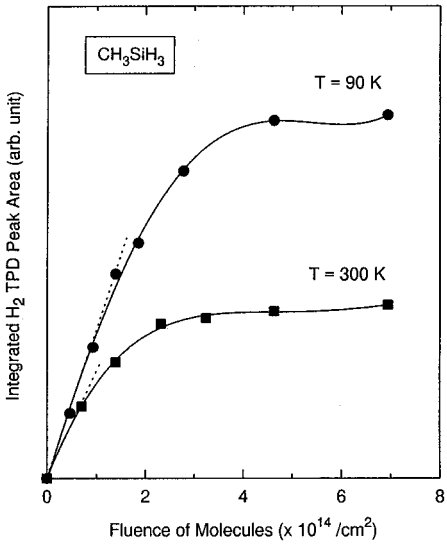

Figure 3. Comparison of CH_3SiH_3 adsorption on Si(100) at 90 and 300 K. The integrated H_2 desorption peak area was used to measure the relative coverage of CH_3SiH_3.

were monitored by the multiplexed mass spectrometer. It was found that H_2 was the only desorption species in the thermal desorption process. Hence, the H_2 yield in thermal desorption is quantitatively related to the coverage of the hydride molecule adsorbed. For Si_2H_6 adsorption at 300 K (Figure 1a), two H_2 desorption features were found with a main desorption peak at ~830 K and a low-intensity shoulder at ~700 K, consistent with the results of other studies.[13−15] The main desorption peak is assigned to monohydride adsorbed species and the shoulder to dihydride adsorbed species produced by molecular decomposition.[13−15] For CH_3SiH_3 adsorption at 300 K (Figure 1b), there is mainly one H_2 desorption peak at ~840 K.

For CH_3SiH_3 and Si_2H_6 adsorption at 90 K (parts c and d of Figure 1), the integrated H_2 temperature-programmed desorption peak area is considerably larger compared to results at 300 K. Since H_2 was the only desorption species, the result indicates that the saturated adsorption coverage of both of these molecules at 90 K is larger than that at 300 K. For Si_2H_6 adsorption at 90 K, the desorption yield of both monohydride and dihydride species increases. For CH_3SiH_3 adsorption at 90 K (Figure 1d), the monohydride peak area increases while a shoulder at ~750 K appears.

The role of the $-SiH_3$ functional group in CH_3SiH_3 adsorption on Si(100) has been studied by comparing the adsorption behavior of C_2H_6, CH_3SiH_3, and Si_2H_6 at 90 K, as shown in Figure 2. Here, the integrated H_2 thermal desorption peak area is used to measure the adsorption coverage. The result shows that C_2H_6 does not stick on Si(100) at 90 K while CH_3SiH_3 and Si_2H_6 molecules have similar sticking coefficients and saturation coverages. The results indicate that the presence of the $-SiH_3$ functional group governs the chemisorption of these molecules on Si(100), since only molecules containing the $-SiH_3$ group are active in chemisorption.

The dissociation behavior of CH_3SiH_3 on Si(100) has been studied by comparing the adsorption coverage at 90 and 300 K. Figure 3 shows the integrated H_2 thermal desorption peak area as a function of CH_3SiH_3 fluence. It is found that at all coverages the integrated hydrogen yield for CH_3SiH_3 adsorption at 90 K is about twice as large as that at 300 K. This comparison suggests that CH_3SiH_3 adsorbs dissociatively on Si(100) at 300 K. The dissociation of a CH_3SiH_3 molecule upon adsorption will produce fragment species that can block more surface sites than the undissociated parent molecule, resulting in lower saturation coverage, as discussed in section IV.

Figure 4 shows a comparison of the carbon Auger intensity observed after adsorption of CH_3SiH_3 onto Si(100) at 300 and 90 K as a function of CH_3SiH_3 fluence. It may by seen that, within our experimental error, the C(KVV)/Si(LVV) intensity ratio for adsorption at 90 K is about twice that observed at 300 K. This confirms the coverage ratio of about 2 obtained from the H_2 desorption measurements for adsorption at 90 and 300 K as shown in Figure 3. The error bars on the last points on each curve correspond to the average deviation obtained in four Auger measurements across the central region of the crystal.

IV. Discussion

A. Preferential Si−C Bond Dissociation of CH_3SiH_3 on Si(100). As deduced from Figures 3 and 4, the saturation coverage of CH_3SiH_3 for adsorption at 300 K is about one-half that obtained for adsorption at 90 K. This indicates that dissociative adsorption occurs at 300 K. The dissociation could be through Si−H, C−H, or Si−C bond scission in the CH_3-SiH_3 molecule.

Steric arguments may be employed to describe the dissociation of the CH_3SiH_3 molecule on Si(100). The upper portion

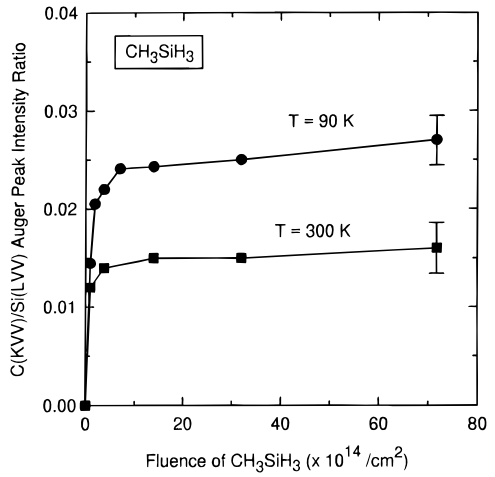

Figure 4. AES study of CH_3SiH_3 adsorption on Si(100) at 90 and 300 K. The C(KVV)/Si(LVV) Auger ratio was used to measure the relative coverage of CH_3SiH_3.

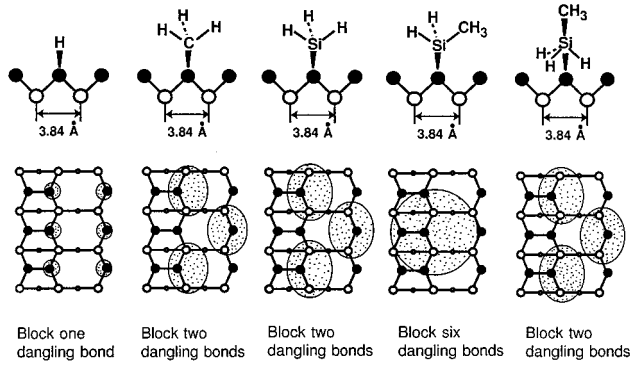

Figure 5. Schematic diagram of the undissociated CH_3SiH_3 molecule and the dissociation products on the Si(100)-(2 × 1) surface. All species are considered to adsorb on the surface dangling bonds.

of Figure 5, in which the surface silicon dimers are viewed end on, shows schematic diagrams of the various adsorbed species that could be derived from CH_3SiH_3 adsorption. In the lower portion of Figure 5, the number of dangling bond sites that could be blocked by the various species is indicated. In this analysis on extended ordered ensembles of surface species, a dangling bond site is considered to be blocked if the van der Waals radius of the chemisorbed neighboring species extends over a neighboring Si atom possessing a dangling bond. A second analysis employs hexagonal close packing of the adsorbed species with their van der Waals radii to calculate the number of these species per unit cell (uc) of Si(100)-(2 × 1) (uc = 29.49 Å^2), and from this the number of dangling bonds blocked by each species may be determined. This second model yields a lower blocking capacity compared to the localized adsorption needed and is probably less realistic than the localized model. These results are summarized in Table 1 for various possibilities.

Both models yield a revealing ratio of the dangling bond blocking capacity of a pair of −CH_3 and −SiH_3 surface species compared to an adsorbed SiH_3CH_3 molecule. In the case of the localized adsorption site model, the blocking ratio is 2; in the case of the close-packing model, the blocking ratio is 1.6. If the SiH_3CH_3 molecule should produce an adsorbed H and an adsorbed SiH_2CH_3, the blocking ratio for the close-packing model is 2.39 and for the localized model the blocking ratio is 3.5. Since the experimental blocking ratio for the dissociated species compared to the undissociated species is ∼2, we conclude that dissociation of the Si−C bond is most likely on steric grounds.

TABLE 1: van der Waals Radii of Different Adsorption Species and Site Blocking

		surface dangling bond sites blocked	
surface species[a]	van der Waals radii (Å)	close packing[b]	adsorbed on the dangling bond sites[d]
−H	∼1.2	0.34	1
−CH_3	∼2.2	1.14	2
−SiH_3	∼2.6	1.59	2
−SiH_2CH_3	∼4.0	3.75	6
−SiH_3CH_3[c]	∼2.7	1.71	2

[a] All species are considered to have cylindrical symmetry about a bond between surface and adsorbed species. The bond lengths employed are C−H = 1.093 Å, Si−H = 1.485 Å, and Si−C = 1.867 Å in CH_3SiH_3.[16] [b] Assumed close packing of adsorbed species on a 29.49 Å^2 unit cell of the Si(100)-(2 × 1) surface. [c] The species is considered to adopt a pentacoordinate configuration, and the van der Waals radius is that of the SiH_3 group along the Si−Si axis. [d] The van der Waals area of localized species is employed to calculate the blocking of dangling bond sites. In this analysis, an extended ordered ensemble of species was used and compared to the underlying Si lattice to calculate the dangling bond blocking capability.

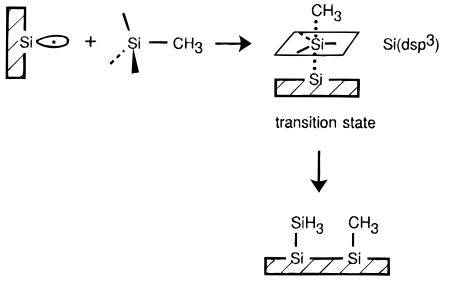

Figure 6. Schematic nucleophilic substitution reaction (S_N2 reaction) of CH_3SiH_3 dissociation on Si(100).

B. Dissociation Adsorption Mechanism of CH_3SiH_3 on Si(100). As suggested by Figures 1 and 2, the −SiH_3 functional group plays a key role in the interaction of CH_3SiH_3 with Si(100). The CH_3SiH_3 dissociation reaction may proceed at 300 K through a mechanism that is similar to the nucleophilic substitution reaction (S_N2 reaction), a well-known reaction mechanism in organic chemistry.[17] In this mechanism (Figure 6), the nucleophilic reagent (the surface atom) attacks the Si atom opposite the leaving group (the CH_3 group), resulting in the formation of a pentacoordinate intermediate and then, following Si−C bond cleavage, a stronger chemical bond is formed between the −SiH_3 group and the surface. In a usual organic S_N2 reaction, the reaction involves a pentacoordinate C atom transition state and has a high reaction barrier.[17] In contrast, for a silicon atom, 3d atomic orbitals are available for bonding so that 5-fold coordination Si compounds are commonly found in the gas phase.[18] The bonding of Si with other atoms is through the dsp^3 orbitals. The ability of silicon to form pentacoordinate compounds lowers the activation energy for bond breaking, as shown by theoretical calculations.[19−20] A similar reaction mechanism has been proposed by Avouris and Boszo[6] for the dissociative Si_2H_6 reaction on Si(111).

C. Pentacoordinate Si Chemisorption State of CH_3SiH_3. The dissociative adsorption of disilane on Si(111) was postulated to occur with a constant sticking coefficient through a molecular precursor state.[13] A similar mechanism may apply to CH_3SiH_3 adsorption on Si(100) at 300 K as shown in Figure 7.

CH_3SiH_3 molecules in the chemisorption state at 90 K may interact with the surface dangling bonds through either the H or Si atom in the −SiH_3 group, since the −SiH_3 group governs the CH_3SiH_3 adsorption on Si(100) as indicated in Figures 1 and 2. Our results suggest that the chemical interaction between

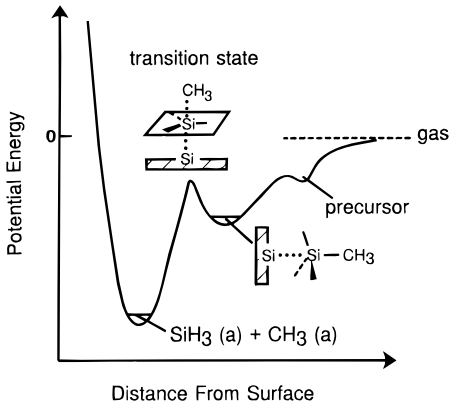

Figure 7. Schematic potential energy diagram of CH_3SiH_3 adsorption and reaction on Si(100). The pentacoordinate Si intermediates are postulated to be involved in the adsorption and dissociation.

the Si atom in the CH_3SiH_3 and the surface is the key factor in CH_3SiH_3 adsorption on Si(100). Charge transfer from the surface to disilane was postulated in a recent theoretical calculation.[22] Thus, it is likely that the silane−surface interaction in the chemisorbed CH_3SiH_3 species is through partial charge transfer from the surface to the Si atom in CH_3SiH_3, which adopts a pentacoordinate configuration as shown in Figure 7.

V. Summary

We have studied the adsorption and reaction behavior of C_2H_6, CH_3SiH_3, and Si_2H_6 on Si(100) using both TPD and AES techniques. Several results have been obtained as follows.

1. Thermal desorption studies indicate that both CH_3SiH_3 and Si_2H_6 molecules have similar adsorption and reaction behavior on Si(100) at both 90 and 300 K.

2. The adsorption of CH_3SiH_3 on Si(100) is governed by the interaction of the $-SiH_3$ functional group with the surface. The interaction is postulated to involve charge transfer from the surface to the Si atom in CH_3SiH_3, which adopts a dsp^3 pentacoordinate configuration.

3. Methylsilane adsorbs dissociatively on Si(100) at 300 K, resulting in a factor of 2 reduction in saturation coverage compared to that at 90 K. The dissociation is postulated to occur through a nucleophilic substitution reaction mechanism, resulting in Si−C bond breakage and the formation of CH_3(a) and SiH_3(a) species.

4. At higher temperatures, both the $-CH_3$ and the $-SiH_3$ groups further decompose on the surface, resulting in the formation of surface-bound monohydride and dihydride species.

Acknowledgment. We acknowledge the support of this research by the Materials Research Center of the University of Pittsburgh.

References and Notes

(1) Golecki, L.; Reidinger, F.; Marti, J. *Appl. Phys. Lett.* **1992**, *60*, 1703.
(2) Liu, C. W.; Sturm, J. C. *Inst. Phys. Conf. Ser.* **1993**, *137*, 83.
(3) Ohshita, Y. *J. Cryst. Growth* **1995**, *147*, 111.
(4) Johnson, A. D.; Perrin, J.; Mucha, J. A.; Ibbotson, D. E. *J. Phys. Chem.* **1993**, *97*, 12937.
(5) Waltenburg, H. N.; Yates, J. T., Jr. *Chem. Rev.* **1995**, *95*, 1589, and references therein.
(6) Avouris, P.; Boszo, F. *J. Phys. Chem.* **1990**, *94*, 2243, and references therein.
(7) Bronikowski, M.; Wang, Y.; McEllistrem, M. T.; Chen, D.; Hamers, R. J. *Surf. Sci.* **1993**, *298*, 50.
(8) Wang, Y. J.; Bronikowski, M. J.; Hamers, R. J. *Surf. Sci.* **1994**, *311*, 64.
(9) Xu, J.; Choyke, W. J.; Yates, J. T., Jr. Submitted for publication.
(10) Nishino, H.; Yang, W.; Dohnálek, Z.; Ukraintsev, V. A.; Choyke, W. J.; Yates, J. T., Jr. *J. Vac. Sci. Technol.* **1997**, *A15*, 182.
(11) Winkler, A.; Yates, J. T., Jr. *J. Vac. Sci. Technol.* **1988**, *A6*, 2929.
(12) Bozack, M.; Muehlhoff, L.; Russell, J. N., Jr.; Choyke, W. J.; Yates, J. T., Jr. *J. Vac. Sci. Technol.* **1987**, *A5*, 1.
(13) Gates, S. M. *Surf. Sci.* **1988**, *195*, 307.
(14) Trapeznikova, I. N.; Kon'kov, O. I.; Chelnokov, V. E.; Terukov, E. I.; Vlasenko, M. P. *Inst. Phys. Conf. Ser.* **1993**, *137*, 125.
(15) Taylor, P. A.; Wallace, R. M.; Cheng, C. C.; Weinberg, W. H.; Dresser, M. J.; Choyke, W. J.; Yates, J. T., Jr. *J. Am. Chem. Soc.* **1992**, *114*, 6754.
(16) Weast, R. C., Ed. *Handbook of Chemistry and Physics*, 69th ed.; CRC: Boca Raton, FL, 1988; pp F167−F169.
(17) March, J. *Advanced Organic Chemistry: Reactions, Mechanisms and Structure*; McGraw-Hill: New York, 1968.
(18) Tandura, S. N.; Voronkov, M. G.; Alekseev, N. V. *Top. Curr. Chem.* **1986**, *131*, 99.
(19) Baybutt, P. *Mol. Phys.* **1975**, *29*, 389.
(20) Dewar, M. J. S.; Healy, E. *Organometallics* **1982**, *1*, 1705.
(21) Baldridge, K. K.; Boatz, J. A.; Koseki, S.; Gordon, M. S. *Annu. Rev. Phys. Chem.* **1987**, *38*, 211.
(22) Pai, S.; Doren, D. *J. Phys. Chem.* **1994**, *98*, 4422.